Electronic structure of metal quinoline molecules from G_0W_0 calculations

A. Droghetti,[1] Mirko Cinchetti,[2] and Stefano Sanvito[1]
[1]*School of Physics, AMBER and CRANN Institute, Trinity College, Dublin 2, Ireland*
[2]*Department of Physics and Research Center OPTIMAS, University of Kaiserslautern, Erwin-Schroedinger Strasse 46, 67663 Kaiserslautern, Germany*

(Received 14 April 2014; revised manuscript received 11 June 2014; published 30 June 2014)

The photoemission spectra of four different metal quinoline molecules, namely, the prototypical tris(8-hydroxyquinolinato)-aluminum(III) (Alq_3) complex and the related compounds Gaq_3, Inq_3, and tris-(9-hydroxyphenalen-1oate)-aluminum(III) [$Al(OP)_3$] are compared to the electronic structure computed with different first-principles methods. In general, we found that, for Alq_3, Gaq_3, and Inq_3, the molecular orbitals obtained with density functional theory and hybrid functionals represent a good approximation to the quasiparticle states. The same conclusion can be partially extended to the interesting case of $Al(OP)_3$, although a direct comparison between theoretical and experimental results appears rather difficult for states, which are lower in energy than the first ten highest occupied molecular orbitals. Taking our results as a starting point we critically discuss the different available experimental data concerning the charge transport gap of Alq_3.

DOI: 10.1103/PhysRevB.89.245137 PACS number(s): 31.15.A−

I. INTRODUCTION

The last few decades have witnessed a rapidly increasing interest in electronic and optoelectronic technologies based on organic semiconductors (OSCs) [1]. Indeed OSCs present several advantages, when compared to their inorganic counterparts: These extend from the ease of their processability to the possibility of chemically modifying, tuning, and improving their properties [2]. Furthermore, in addition to electronic applications, recently there has been a considerable research effort aiming at exploiting OSCs in spintronic devices [3–5]. This follows from the observation that OSCs are mainly composed of light elements so that the spin-orbit coupling is considered weak and a very long spin-relaxation time is expected [6]. Therefore, if efficient spin injection from ferromagnetic metals into OCSs is achieved [7], multifunctional OSCs will provide novel opportunities for technology applications.

The tris(8-hydroxyquinolinato)-aluminum(III) complex, in short Alq_3, is one the most studied among the various OSCs, as it represents the workhorse material for organic light-emitting diodes (OLEDs) as well as for spin-valve devices. In addition to Alq_3, novel metal quinoline complexes have been recently synthesized. These include the Gaq_3, Inq_3 [8,9], and the tris-(9-hydroxyphenalen-1oate)-aluminum(III) [in short $Al(OP)_3$] molecules [10] (see Fig. 1 for a ball and stick diagram). While Gaq_3 and Inq_3 are obtained from Alq_3 by chemically substituting Al with either Ga or In, the $Al(OP)_3$ complex has the same metal center as Alq_3, but it is characterized by much larger ligands bonded to the Al^{3+} ion only via oxygen donors.

Gaq_3 and Inq_3 have been already utilized in OLEDs [11,12] and, moreover, they were recently proposed as interesting systems for spintronics. In fact, in this context, they were first studied in order to understand how the spin-orbit strength affects the spin-relaxation time [8], and secondly, in order to inspect whether the different metal center alters the electronic and magnetic properties of the interface with cobalt [9]. In contrast, $Al(OP)_3$ has been investigated because the large ligands are expected to improve the spin-filtering effect at a ferromagnet/molecule interface [10] as well as the mobility in the bulk with respect to the case of Alq_3 [13].

To date, several theoretical studies have discussed the electronic structure of Alq_3 by using density functional theory (DFT) calculations [14–16]. These show that the density of (occupied) states (DOS) computed with the generalized gradient approximation (GGA) to the exchange-correlation functional is able to reproduce reasonably well the ultraviolet photoemission (UPS) spectrum. However, several remarkable differences between the measured UPS spectrum and the calculated GGA DOS can be noted [16]. These mainly concern the incorrect position of the highest occupied molecular orbital (HOMO), in the absence of a shoulder near the second HOMO (clearly visible in experiments), and in a general compression of the entire DFT spectrum.

Although, in (exact) DFT, the identification of the Kohn-Sham (KS) spectrum with the UPS spectrum is not rigorously justified other than for the HOMO energy (through the "ionization potential theorem") [17–20], practically the KS eigenenergies are often found to represent a good zeroth-order approximation to experiments (a detailed discussion about this subject can be found in Ref. [21]). Furthermore, in the case of OSCs, most of the shortcomings of the DFT-GGA occupied spectrum can be related to the self-interaction error (SIE) [22], i.e., the spurious interaction of an electron with the potential generated by itself [23]. In fact, for Alq_3, a much improved agreement between the DOS and UPS spectrum can be recovered by using hybrid functionals [16], in which part of the SIE is effectively corrected for by mixing a percentage of exact Hartree-Fock exchange with a semilocal one [24]. Note that in Ref. [16] a screened-exchange approach was used in order to correct for the SIE in the occupied molecular states; however, it was recently demonstrated that the long-range part of the exchange is important for describing the electron addition/removal energy in molecules [25–28].

In two recent studies [9,10], we have compared the UPS spectra of all the above-mentioned compounds [Alq_3, Ga_3, Inq_3, and $Al(OP)_3$] with the DFT DOS. In the case of Alq_3, we have further verified that a fairly accurate DOS for the occupied states can be obtained by correcting for the SIE with either hybrid functionals or with the atomic self-interaction correction (ASIC) scheme [29,30], which was

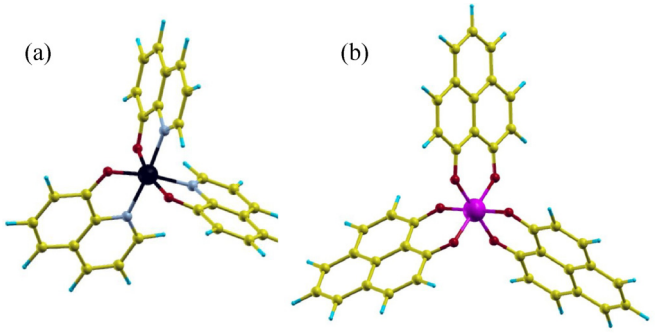

FIG. 1. (Color online) Mq_3 (M = Al, Ga, and In) molecule (a) and $Al(OP)_3$ molecule (b). Color code: C = yellow, O = red, N = gray, H = blue, Al = purple, and M = Al,Ga,In = black.

previously successfully applied to the description of other molecules [31–33]. Similarly, these methods also provide a good description of the occupied spectrum for Gaq_3 and Inq_3, where, *de facto*, the valence states of the metal center do not contribute to the frontier orbitals so that their DOS is almost identical to that of Alq_3. In contrast, in the case of $Al(OP)_3$, some notable differences between the theoretical and the experimental spectrum were still found even if the SIE was partially accounted for. The issue of the origin of these (and other finer) differences between theoretical and experimental results remains unsolved and we have not been able to clarify whether these originate from the limitation of DFT/hybrid-DFT or from some effects not considered in the calculation (for example, slightly different conformation of the molecule in thin films, vibrational effects, or high-order scattering processes).

In order to improve our understanding of the (occupied and unoccupied) spectrum of metal quinoline complexes, we present here the results of calculations performed with the G_0W_0 method. This is based on the GW approximation of the many-body perturbation theory [34–37], where in order to limit the computational cost, the Green function and the screened Coulomb interaction entering into the self-energy are constructed with the underlying KS eigenvalues and eigenstates. Then, the quasiparticle excitation energies are evaluated as the first-order perturbative correction to the KS eigenvalues. The G_0W_0 scheme relies on the assumption that the KS wave functions are a good zeroth-order approximation for the real quasiparticle wave functions, so that the difference between the self-energy and the DFT exchange-correlation potential can be treated as a small perturbation. Although this approximation may be considered often too drastic, practically G_0W_0 has become one of the most appealing electronic structure methods for going beyond DFT and it has provided quite satisfactory results for both solids [34,37–39] and molecules [40–47]. In particular, in several works [41,45,47,48], it was discussed how G_0W_0 yields excellent results when the generalized KS orbitals obtained with a hybrid functional are used as a starting point for the perturbative calculation. This then suggests that the effective correction for the SIE error at the DFT level is reflected in more accurate perturbative quasiparticle energies. Furthermore, a similar conclusion was recently reached by Marom *et al.* [49], who after exploring the entire range of GW-based schemes, explained the success of the G_0W_0 approach combined with hybrid DFT as a "fortunate error cancellation." In this the DFT incorrect screening, due to the underestimated gap between the HOMO and the lowest unoccupied molecular orbital (LUMO), compensates for neglecting the vertex corrections.

Our paper is organized as follows: First we describe the computational methods used (Sec. II). Then, we present the results of our DFT and G_0W_0 calculations for all four molecules considered (Sec. III); these results are systematically compared with UPS spectra from Refs. [9,10]. Next, we present a critical discussion about the determination of the transport gap for Alq_3 (Sec. IV); this represents the key quantity for the interpretation of the experimental results in both organic optoelectronics as well as spintronics. Finally we conclude (Sec. V).

II. COMPUTATIONAL METHODS

All the calculations were performed by using the FHI-AIMS all-electron code [50,51]. FHI-AIMS employs numerical atom-centered orbitals (NAO). These can be systematically improved beyond the minimal basis for the free-atom-like radial orbitals by adding further radial functions, which are grouped in four sets labeled "tiers 1–4." The molecular geometries were optimized until the ionic forces were smaller than 0.01 eV/Å by using DFT with the Perdew, Burke, and Ernzerhof (PBE) GGA for the exchange-correlation functional [52,53]. A tier 2 basis set was used. The effective one-component (i.e., zero coupling between the two spin channels in a collinear calculation) scalar relativistic approximation called "atomic-ZORA" (zeroth-order regular approximation) [50] was applied for treating relativistic effects.

G_0W_0 calculations were carried out by using the (generalized)-KS orbitals and eigenvalues obtained with both PBE and the nonempirical hybrid functional PBE0, which includes 25% of Hartree-Fock exchange [54] (in accordance with the standard practice [49], we will use the notation G_0W_0@PBE and G_0W_0@PBE0 in order to specify the starting point for the G_0W_0 calculation). In order to include relativistic effects, in addition to the atomic-ZORA, also a second method, the scaled-ZORA [55], was tested for the "single-point" DFT calculation that served as staring point for the G_0W_0 method. However, the results were found not to depend on the two possible choices within the accuracy required in this study. By performing a basis set converge test for the ionization potential (IP) of Alq_3, we verified that the difference between the tier 1 and the tier 2 value is about 0.34 eV, while the difference between the tier 2 and the tier 3 value is 0.1 eV, and finally, the difference between the tier 3 and the tier 4 value is only 0.05 eV. This is in agreement with previous studies by other authors [47,49,51,56]. A similar trend was also found for the electron affinity (EA). Furthermore, the order of the frontier molecular orbitals and the spacing between the molecular levels was found not to change qualitatively when going from tier 2 to tier 3 and from tier 3 to tier 4. As previously pointed out by Marom *et al.* [49], the G_0W_0 tier 2 spectrum usually differs from the G_0W_0 tier 4 spectrum only by a rigid shift of less than 0.2 eV. Some qualitative differences between the tier 2 and the tier 4 spectra were found only for unoccupied states, which are about 3 eV far above the LUMO energy. However, these states

are not relevant for this study. Therefore, all results presented in this paper have been obtained at the tier 2 level with the understanding that it provides converged enough spectra for our purposes.

FHI-AIMS calculates the *GW* self-energy on the imaginary frequency axis. We have verified that, by increasing the number of imaginary frequency points beyond the default value (which is equal to 80) [57], the results do not substantially change. The two-pole fitting [58] is used for the analytic continuation of the self-energy to the real axis.

Finally we note that FHI-AIMS allows one to carry out calculations without imposing periodic boundary conditions thus avoiding periodic-image-related effects.

III. DFT AND G_0W_0 RESULTS

The UPS spectra, the (generalized) KS eigenvalues, the G_0W_0 quasiparticle energies, and the related DOS for the occupied states of Alq_3, Gaq_3, Inq_3, and $Al(OP)_3$ are displayed in Figs. 2–5, respectively (from now on the notation Mq_3 will be used in order to generally indicate the three molecules Alq_3, Gaq_3, and Inq_3). The UPS spectra are extracted from Refs. [9,10], where they were measured for the surface layer of a 4- to 5-monolayer (ML)-thick film deposited on cobalt [1 ML $Alq_3 \approx 1.3$ nm, 1 ML $Al(OP)_3 \approx 1.5$ nm]. All the UPS spectra are presented after subtraction of the secondary electron background by using the procedure described in Ref. [59]. Here, these spectra have been rigidly shifted in order to line up the zero-energy value with the vacuum level instead of the molecule/substrate-interface Fermi level. As discussed in Refs. [9,10], the molecular films used in the UPS experiment were thick enough to suppress photoemission from the substrate. In the case of Alq_3 this is further confirmed by the fact that the shape of the UPS spectrum presented here appears identical to that reported for 30 ML Alq_3 on Si(100)

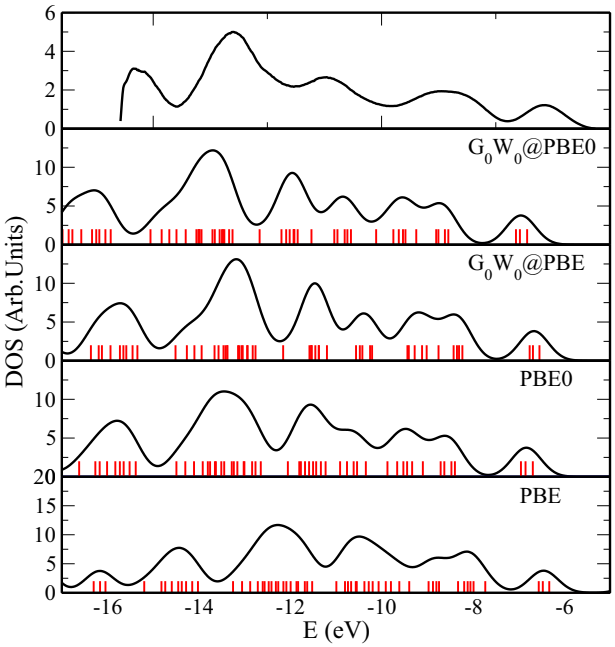

FIG. 3. (Color online) Gaq_3 UPS spectrum (top panel) compared to the occupied DOS computed with PBE, PBE0, G_0W_0@PBE, and G_0W_0@PBE0. A Gaussian broadening of 0.35 eV has been added to the theoretical DOS. The red vertical bars indicate the energy of each quasiparticle/(generalized-)KS eigenstate.

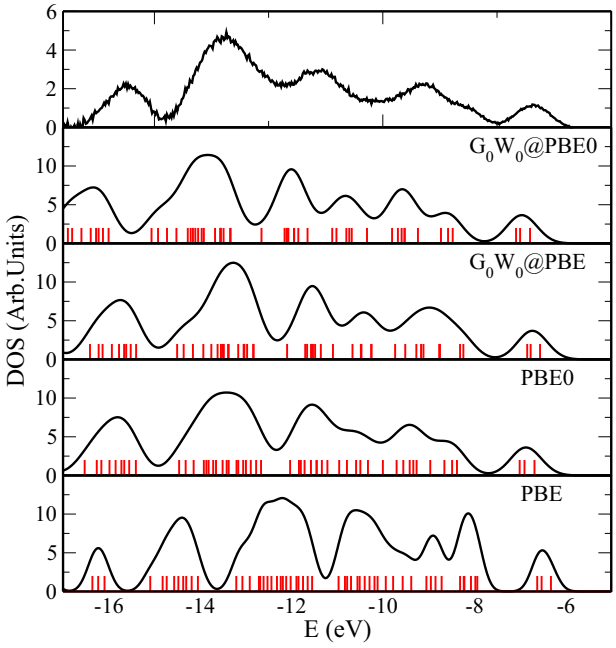

FIG. 2. (Color online) Alq_3 UPS spectrum (top panel) compared to the DOS computed with PBE, PBE0, G_0W_0@PBE, and G_0W_0@PBE0. A Gaussian broadening of 0.35 eV has been added to the theoretical DOS. The red vertical bars indicate the energy of each quasiparticle/(generalized-)KS eigenstate.

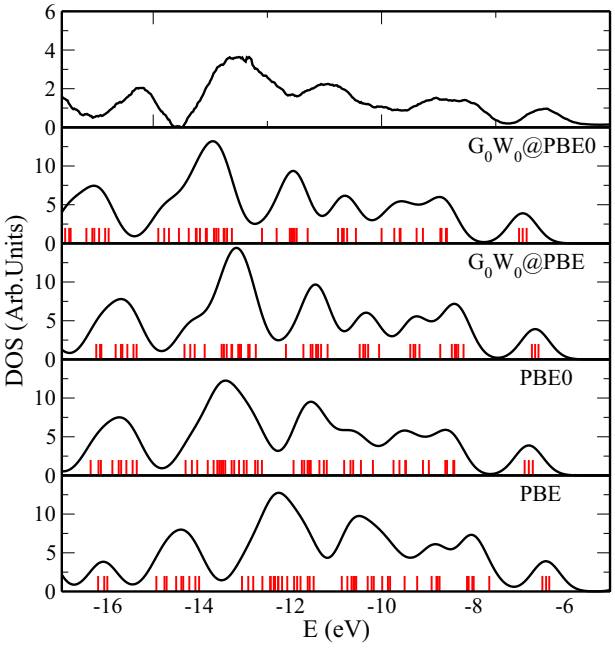

FIG. 4. (Color online) Inq_3 UPS spectrum (top panel) compared to the occupied DOS computed with PBE, PBE0, G_0W_0@PBE, and G_0W_0@PBE0. A Gaussian broadening of 0.35 eV has been added to the theoretical DOS. The red vertical bars indicate the energy of each quasiparticle/(generalized-)KS eigenstate.

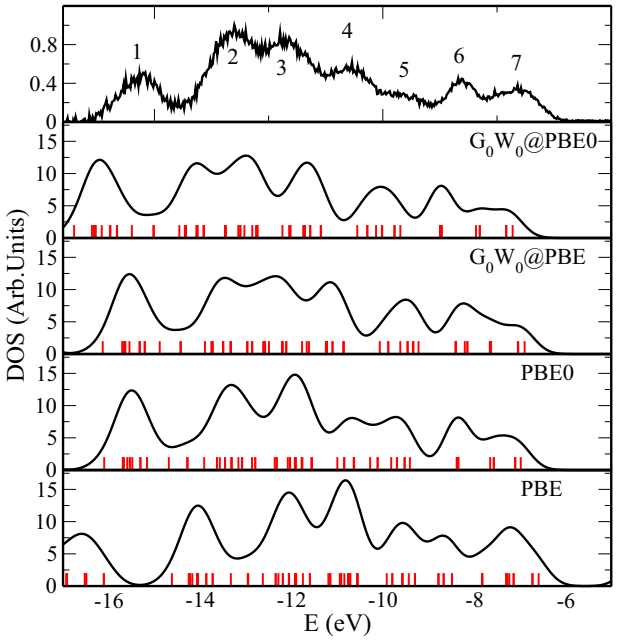

FIG. 5. (Color online) $Al(OP)_3$ UPS spectrum (top panel) compared to the occupied DOS computed with PBE, PBE0, G_0W_0@PBE, and G_0W_0@PBE0. A Gaussian broadening of 0.35 eV has been added to the theoretical DOS. The red vertical bars indicate the energy of each quasiparticle/(generalized-)KS eigenstate. See the main text for the numbering in the top panel.

[15], for 46 ML Alq_3 on SiO_2 [16], and for 4–8 ML Alq_3 on gold [60]. Unfortunately, to our knowledge, the gas-phase UPS spectrum is not available even for Alq_3. In general, one expects the orbital energies of molecules on the top layer of a film to be rigidly shifted with respect to the corresponding energies for the gas phase. This shift is due to the polarization induced on the surrounding molecules by the photoinduced hole [61]. It tends to decrease the IP, to increase the EA, and to displace rigidly occupied and unoccupied states accordingly [60,62,63]. Therefore, as we will discuss in more detail in the following section, some care is in general needed when trying to match the theoretical energies for frontier orbitals with the UPS data at hand.

The PBE (PBE0) DOS and the (generalized) KS eigenvalues were shifted in order align the HOMO energy with the IP, computed with the ΔSCF method [64] and according to the formal definitions $IP = E(N-1) - E(N)$, where $E(N)$ and $E(N-1)$ are the total DFT energy of the neutral molecule and of the cation, respectively. This is the proper way for calculating the IP from DFT. In fact, although in exact DFT the HOMO energy is the negative of the IP [17–20], this does not happen when an approximate exchange-correlation functional is employed. Similarly, the EA has also been calculated with the ΔSCF scheme and by using the formal definition $EA = E(N) - E(N+1)$ [where $E(N+1)$ is the total DFT energy for the anion]; the results for both IP and EA are reported in Table I. In contrast to previous calculations [9,10], where the *adiabatic* IP and EA were presented, we have here computed the *vertical* IP and EA, i.e., the geometries of the neutral molecule and of the singly charged ion are assumed to be the same. This is because the G_0W_0 spectrum, which is used for comparison, does not account for any ionic relaxation effect. Furthermore, and more importantly, the ionic relaxation is generally too slow to contribute to the photemission and in any case this effect is quite small. In fact the differences between the vertical and the adiabatic IP and EA, computed with PBE, turn out to be only 0.06 and 0.13 eV for Alq_3 (and almost identical for the other compounds). Very similar results were also found by Curioni *et al.* [14] with another GGA functional.

TABLE I. (Vertical) ionization potential (IP) and electron affinity (EA) computed with the various electronic structure methods. All data are in eV.

	Method	IP	EA
Alq_3	ΔSCF(@PBE)	6.34	1.16
Alq_3	ΔSCF(@PBE0)	6.78	0.81
Alq_3	G_0W_0@PBE	6.56	1.05
Alq_3	G_0W_0@PBE0	6.78	0.81
Gaq_3	ΔSCF(@PBE)	6.33	1.15
Gaq_3	ΔSCF(@PBE0)	6.69	0.86
Gaq_3	G_0W_0@PBE	6.55	1.02
Gaq_3	G_0W_0@PBE0	6.81	0.81
Inq_3	ΔSCF(@PBE)	6.30	1.17
Inq_3	ΔSCF(@PBE0)	6.61	0.93
Inq_3	G_0W_0@PBE	6.57	0.99
Inq_3	G_0W_0@PBE0	6.83	0.76
$Al(OP)_3$	ΔSCF(@PBE)	6.59	1.89
$Al(OP)_3$	ΔSCF(@PBE0)	6.98	1.63
$Al(OP)_3$	G_0W_0@PBE	6.90	1.65
$Al(OP)_3$	G_0W_0@PBE0	7.16	1.41

In contrast to the DFT case, the orbital energies computed with G_0W_0 represent the (approximate) quasiparticle energies of a system. Therefore the IP and the EA, which are also reported in Table I, are directly identified as the opposite of the G_0W_0 HOMO and LUMO energies. We note that the DFT-ΔSCF IP and EA are usually very close to the G_0W_0 ones, when these are computed with the same functional as the starting point. Then, for all cases, the G_0W_0 IP (EA) is about 0.2 eV (0.1 eV) larger (smaller) than the ΔSCF IP (EA).

If the computed values for IP were blindly compared to the experimental estimates [$IP^{exp} = 6.4$ eV for Mq_3 [9] and $IP^{exp} = 6.9$ eV for $Al(OP)_3$ [10]], we would infer that G_0W_0@PBE0 and ΔSCF(@PBE0) return a too large IP, while G_0W_0@PBE and ΔSCF(@PBE) appear to perform better. However, as mentioned above, the experimental IPs were measured with UPS for the top layer of a film and these values are likely to be smaller than that for the gas-phase molecule. In absence of gas-phase data, the comparison between the experimental and the theoretical estimates for IP turns out to be quite problematic and it requires some care. We will return to this issue in the next section, where an extensive discussion will be presented.

In Table II, we report the so-called the "quasiparticle gap" or the "transport gap" (TG) of all four compounds. The TG is defined directly as the difference between the LUMO and the HOMO energies and it can be obtained simply from the G_0W_0 quasiparticle energies or, in (hybrid) DFT, from the difference between the ΔSCF IP and the EA (we remind one

TABLE II. Transport gap (TG) for the four compounds computed with the different methods. All data are in eV.

Method	Alq_3	Gaq_3	Inq_3	$Al(OP)_3$
ΔSCF(@PBE)	5.18	5.18	5.13	4.7
ΔSCF(@PBE0)	5.8	5.83	5.68	5.35
G_0W_0@PBE	5.51	5.53	5.58	5.25
G_0W_0@PBE0	5.97	6	6.07	5.75

that TG must not be confused with the optical gap measured in absorption experiments, which is usually smaller by an amount defined by the exciton binding energy [65]). We note that, for all four compounds, ΔSCF(@PBE) always returns the smallest estimates for TG, while G_0W_0@PBE0 the largest, with an energy difference between the two of about 1 eV. Unfortunately, to our knowledge, no experimental value for the TG of Gaq_3, Inq_3, and $Al(OP)_3$ is available to compare our results with, while a detailed discussion about the Alq_3 case is presented in the next section.

Next, we compare the calculated DOS with the UPS results. In the case of Alq_3 (see Fig. 2), we note that the first peak in the UPS spectrum, which in experimental studies is usually identified with the HOMO, in reality originates from three very closely energy-separated molecular orbitals located on the phenoxide moiety [9,14]. PBE is able to describe this feature as well as the other more advanced methods. In contrast, PBE is not able to provide a satisfactory description of the spectrum in the energy range just below the HOMO, which extends from about −7 to −10 eV in the UPS spectrum. In fact, while the PBE DOS presents a two-peak structure, the UPS spectrum has a single peak centered at about −9 eV, which is anticipated by a shoulder at about −8 eV. As previously pointed out [16], the use of a hybrid functional (in our specific case, PBE0) improves the overall DOS, by correcting for the SIE in the same way as other approximate correction schemes would [9]. Then the "'peak+shoulder" feature is reproduced. Interestingly, G_0W_0@PBE is not fully able to "repair" the incorrect PBE DOS, although it strictly refines upon this by systematically stretching the entire spectrum. Finally G_0W_0@PBE0 resolves very clearly the shoulder at around −8 eV and the overall DOS looks in very good agreement with the UPS spectrum.

The electronic structures of Gaq_3 and Inq_3 are very similar to that of Alq_3 as the metal ions have only a negligible contribution to the orbitals with a binding energy within several eV away from the HOMO [9]. Therefore, not surprisingly, very similar conclusions concerning the performances of the different methods can be drawn also for these systems. We note, however, that the UPS spectra of Inq_3 and Ga_3 do not present the shoulder at around −8 eV, but they rather have an almost 2 eV-broad peak. Once again PBE0 and G_0W_0@PBE0 return a good agreement between the theoretical and experimental spectra.

In summary, our results for Mq_3 are very similar to those reported for other OSCs [47,49]: The best results are achieved by using G_0W_0@PBE0, but PBE0 mimics the occupied quasiparticle spectrum and corrects for most of the shortcomes of PBE.

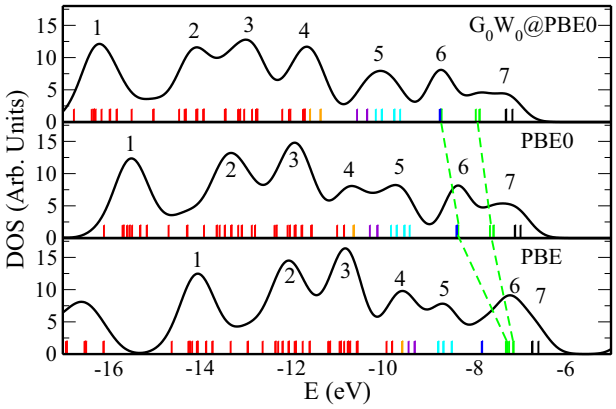

FIG. 6. (Color online) $Al(OP)_3$ DOS and quasiparticle/(generalized-)KS energies computed with G_0W_0@PBE0 (upper panel), PBE0 (middle panel), and PBE (lower panel). The states discussed in the main text are indicated through colored bars. The dashed green line illustrates how the HOMO-6, HOMO-7, and HOMO-8 shift in energy when going from the PBE to the PBE0 and finally to the G_0W_0@PBE0 description of the molecule electronic structure.

Let us now consider the $Al(OP)_3$ molecule, whose DOS and UPS spectrum are displayed in Fig. 5. We note that PBE is clearly unable to reproduce the experimental data: Not only does the PBE DOS appear very "contracted" with respect to the UPS spectrum, but it also differs qualitatively in the energy interval between −10 and −6 eV. In fact, the PBE DOS presents a very wide peak centered at about −7 eV, while the UPS spectrum shows a sharper peak at about −8.5 eV, which follows a very broad shoulder extended over a 2 eV energy range (from about −6 to about −8 eV). Furthermore, the almost flat and featureless region, which goes from about −8.5 eV to −10 eV in the UPS spectrum is substituted, in the PBE DOS, by a relatively narrow peak, which is found at higher energies (about 8.5 eV). In contrast, the agreement between the PBE0 and the G_0W_0 DOS with the UPS spectrum is unequivocally better: These methods reproduce the main features between −6 and −8.5 eV (broad shoulder plus peak). However, in the energy interval between about −8.5 and −11 eV, PBE0 and G_0W_0 return quite different results. On the one hand, the PBE0 DOS presents two broad peaks, which almost merge together. On the other hand, the G_0W_0 spectrum is characterized by a single broad peak centered at about −10 eV, while the next peak is located at about −12 eV and it appears higher and sharper (we note that there are only fine quantitative differences between the G_0W_0@PBE and the G_0W_0@PBE0 results). It is therefore difficult to establish with certainty which of these DOS better reproduce the flat region and the peak centered at about −10.5 eV, which are visible in the UPS spectrum. In order to understand the shortcomings of the different methods in the case of $Al(OP)_3$, it is convenient to look at how the single-particle energy of each molecular orbital is displaced when the various theoretical approaches are considered. In Fig. 6 the DOS and the quasiparticle/(generalized-)KS molecular orbital energies (colored bars) computed with the different methods are presented (the G_0W_0@PBE results are not discussed since they do not differ qualitatively from the G_0W_0@PBE0 ones).

The most relevant features in the DOS have been labeled with progressive numbers (the same numbering is also reported in Fig. 5 in order to facilitate the comparison with the experimental UPS).

First, we focus on the peaks 6 and 7. We note that the *relative* energy position of the first three occupied states, namely, the HOMO and the degenerate HOMO-1 and HOMO-2 (black bars in Fig. 6), is almost the same with PBE, PBE0, and G_0W_0@PBE0. These three states are fully delocalized on the ligands (see Fig. 7, states 1, 2, and 3) so that, according to the standard arguments, the SIE should be small and even PBE is able to provide a fairly good description. In contrast, when we consider the next six states (green bars in Fig. 6), which have a very small energy separation with PBE, we find that PBE0 and G_0W_0@PBE0 push three of them (HOMO-6, HOMO-7, and HOMO-8) down in energy more drastically than the other three (HOMO-3, HOMO-4, and HOMO-5); the shift of these states is clearly highlighted in Fig. 6. Then the three split states end up in an energy region where the other three states (HOMO-9, HOMO-10, and HOMO-11) are already present (blue bars in Fig. 6) so that the coexistence of these six states in the very same energy position, results in the sharp peak 6 in the PBE0 and G_0W_0@PBE0 DOS, while the three states left at a higher energy contribute, together with the HOMO, HOMO-1, and HOMO-2, to form the plateau (feature 7) proceeding that peak. Again, this can be understood in terms of SIE: The states which move down the most in energy when using PBE0 and G_0W_0, are strongly localized only on the oxygen atom surrounding the Al ion (see Fig. 7, states 7, 8, and 9) and therefore present a large SIE. G_0W_0@PBE0 and PBE0 correct for the SIE so that these states are dragged toward lower energies.

Secondly, we consider the group of six states, which are displayed through cyan bars in Fig. 6 (HOMO-12 to HOMO-17). Each of these states presents a very different degree of localization: Some states are fully delocalized over the three ligands, others are fully localized on the oxygen atoms, and several others are in between these two extreme cases (see Fig. 7, states 13–18). Then, when either PBE0 or G_0W_0@PBE0 is employed, each state is displaced with respect to its PBE-computed energy position in a very different way depending on the amount of localization. This results in an overall increase in energy separation compared to the PBE case. Even more importantly, those states, which show the largest localization, are displaced the most and get very close in energy to the next group of three states (HOMO-18, HOMO-19, and HOMO-20, which are represented by the purple bars in Fig. 6). These latter states, in contrast, present a much less pronounced energy shift. Finally such selective shift in energy leads to the assembly of a total of nine states (with an average energy separation of 0.15 eV) within a relatively broad energy interval.

Next, we focus on the following group of three states (HOMO-21, HOMO-22, and HOMO-23), represented by the orange bars in Fig. 6. Although the electron density of these states has a contribution from all three ligands (see Fig. 7, states 22, 23, and 24), these states have clearly no π-conjugated nature. Then we see that PBE0 slightly increases the separation with the previous group of states. In contrast G_0W_0@PBE0 drives these states toward much lower energies and it further splits one of them from the others.

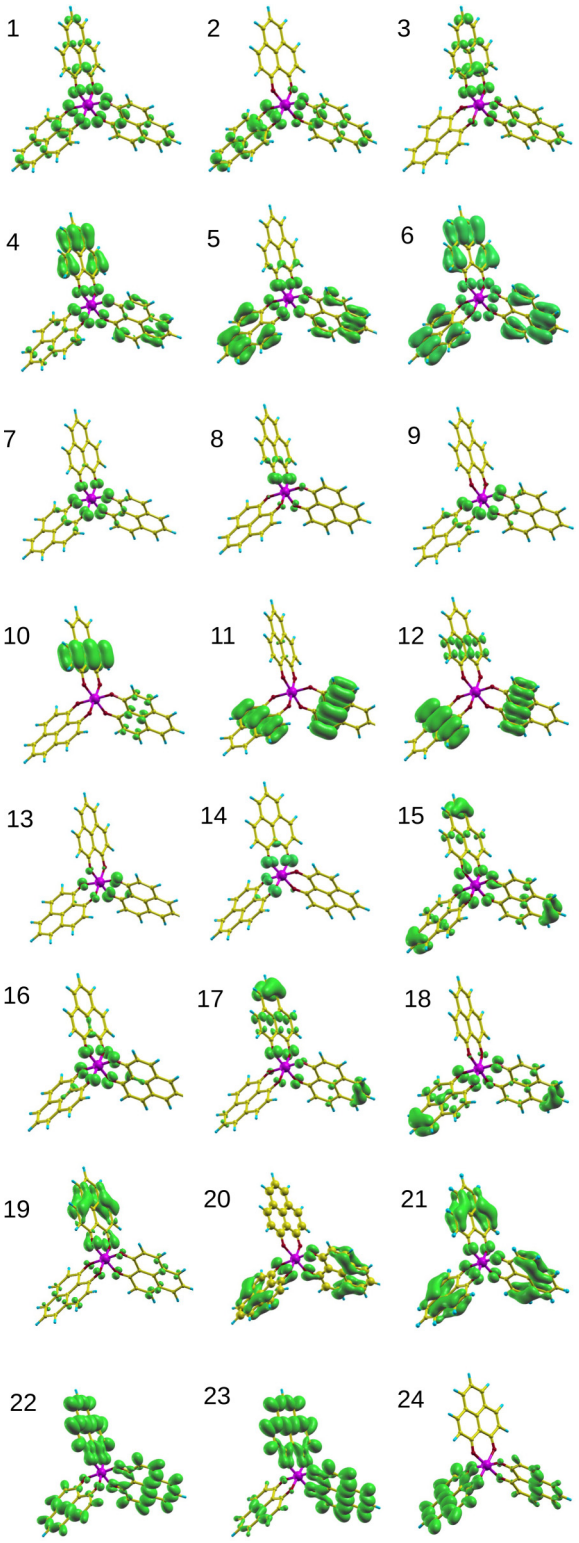

FIG. 7. (Color online) Electron density for the first 24 occupied molecular orbitals of $Al(OP)_3$. The state 1 is the HOMO, while the state 24 is the HOMO-23. Color code: C = yellow, O = red, N = gray, H = blue, and Al = purple. The electron density isosurface is represented by the green bubbles.

Finally, when we look at the states with lower energies than the HOMO-23 (indicated through the red bars in Fig. 6),

we observe that the PBE0 single-particle energy spectrum appears to be very much the same as the PBE one (it looks just slightly stretched), while this is not the case for the G_0W_0@PBE0 spectrum. A detailed investigation concerning these low energy states is very complex and beyond the aim of this work, nevertheless the analysis performed up to this point allows us to understand the main difference from the computed PBE0 and G_0W_0@PBE0 DOS in the energy region we are interested in. On the one hand, the peaks 4 and 5 in the PBE and PBE0 DOS are the very same, but their relative height and separation results from the shift of the relevant states; such shift can be easily explained through arguments related to the SIE. On the other hand, while the peak 5 in the G_0W_0@PBE0 DOS is formed by the HOMO-12, -13, . . . and -20, which have energies similar to those calculated with PBE0; the peak 4 has a different nature. In fact it results from a drastic downshift of the HOMO-21, HOMO-22, and HOMO-23, and of a few other states close in energy; these states then tend to merge together with another group of states forming the peak 4. Unfortunately, a comparison of the theoretical DOS with the UPS data is not able to provide a clear answer about which method performs better. This analysis is further complicated by the fact that each peak in the UPS spectrum results from the contribution of many states and it presents a large broadening, which is due, other than to many-electron and phonon effects, also to the amorphous nature of the molecular layers used for the measurements. This contrasts the typical situation investigated in previous similar studies [21,41,49] in which the considered molecules were composed of few atoms, gas-phase UPS spectra were generally available, and each peak in the UPS spectra could be directly related to one single quasiparticle state or to a group of a few (almost) degenerate states. In addition, for the present case, we note that various DOS, computed with different methods, can display very similar features in a certain energy region, although the single-particle energy spectra are different. This is, for example, the case of the peaks 2 and 3 in the UPS spectrum, which can be easily related to the peaks 2 and 3 in both the PBE0 and G_0W_0@PBE0 DOS, but the two eigenenergies spectra are arguably rather different.

Summarizing, for $Al(OP)_3$, we are not able to benchmark the performances of the different methods for states other than the first ten HOMOs. Nevertheless, for these states, we can conclude uncontroversially that PBE0 performs as well as G_0W_0. As these states are the most relevant in order to understand the chemical and the physical properties of the compound, PBE0 may represent a valuable alternative to G_0W_0.

IV. THE Alq_3 TRANSPORT GAP

After having described the spectra of all four compounds, we now discuss the important issue concerning the Alq_3 TG. In fact there is, in the literature, a large set of theoretical and experimental values, which might look inconsistent at first glance, and here, we provide a critical review of those data.

A common way to extract the TG is by combining UPS and inverse photoemission spectroscopy (IPS) in order to access occupied and unoccupied molecular states, respectively. In this case, there are two ways to proceed [66]: (1) take the energetic distance between the HOMO and the LUMO peak *maxima*, or alternatively, (2) the distance between the peak *onsets* (see the schematic illustration in Fig. 8). Clearly, since the peaks corresponding to the molecular orbitals have typical widths of several hundreds of meV, the first method will always yield a larger TG than the second, with differences up to more than 1 eV [66]. Furthermore, UPS and IPS performed on thick organic films (coverage of more than 3–4 ML), are mainly sensitive to the surface organic layer, as their probing depth is limited by the very short electron mean free path (in the 1 ML range). An alternative way for measuring the TG is via scanning tunneling microscopy (STM) experiments. In contrast to UPS and IPS measurements, STM experiments are typically performed either on (sub-) monolayer-thick samples or by penetrating the tip into the thicker organic layer. In both cases one obtains information about the potential barrier for charge injection directly at the metal/organic interface. However, while by penetrating the tip one probes the interface buried underneath an organic film, in the case of (sub-)monolayer samples one investigates the "naked" interface, whose properties can also be addressed in photoemission experiments performed on very thin organic films (1 ML coverage). Finally and very importantly, UPS and IPS are *laterally averaging* techniques (the probed region is given by the spot size of the light source, which is typically in the micrometer-to-millimeter range), but STM probes the *local* electronic structure directly under the scanning tip.

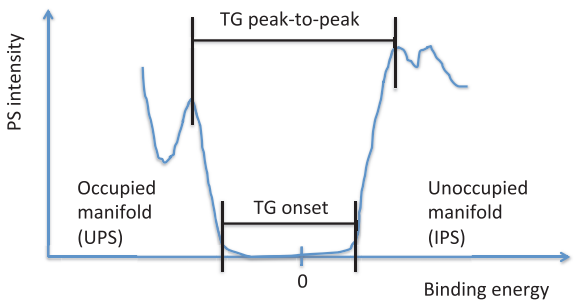

FIG. 8. (Color online) Schematic sketch describing the two different common ways to determine the TG from combined UPS and IPS measurements (peak *maxima* vs peak *onsets*).

We can now discuss the experimental data for the TG of Alq_3 reported in the literature and compare them to our theoretical values. The experimental TG for the surface layer of a thick film, measured by combining UPS and IPS was given as 5.4–5.6 eV [60,66], when evaluating the distance between the HOMO and the LUMO peak maxima, and as 3.64 eV [66,67] by taking the onset distance. Scanning tunneling microscopy experiments, in which the tip penetrates into an Alq_3 film on gold gave an even smaller TG value, equal to 2.96 eV [68,69]. Interestingly, in this second set of experiments, the actual measured TG appears to depend sensitively on the position of the tip with variations of up to 0.7 eV. Although the theoretical values for TG in Table II appear quite close to the estimates, which are obtained with UPS/IPS by looking at the peak maxima, we think that this experimental procedure overestimates the Alq_3 TG (however, this is quite reliable for other molecules).

First, we note that our calculated values in Table II refer to the gas phase and they need to be renormalized in order to account for the medium polarization. Although important progress has been recently made concerning the first-principles theoretical description of these polarization effects in the case of both molecules in perfect crystals [32,70–72] and on surfaces [73–75], the methods at hand can-not be easily applied to the specific case of Alq_3, whose condensed phase is generally amorphous. Therefore, here, we limit the discussion in order to provide a reasonable estimate for the TG renormalization based on the available experimental data. In particular, in Ref. [60] it was proposed that the Alq_3 IP, measured for the surface layer of a thick Alq_3 film, is about 0.75 eV smaller than the Alq_3 gas-phase IP. If we guess that a symmetric shift will increase the EA by a similar amount, we will end up concluding that the TG renormalization is of about 1.5 eV. A comparable estimate has been suggested in Ref. [62] by using empirical and intuitive arguments (in Ref. [62] the TG renormalization is also discussed for molecules isolated on a metallic surface and deep in the bulk of the crystal). Thus, after assuming that those values represent at least the correct figure of merit for the size of the IP and EA renormalization, we argue that TG for Alq_3 molecules *on a film surface* is in between 3.5 and 4.5 eV so that the experimental values inferred from the UPS and IPS peak maxima are too large. In addition, we note that the assumption that polarization effects cannot be neglected is in line with the UPS measurements reported in Ref. [76], where the HOMO of Alq_3 was found to shift by 0.3 eV to higher binding energies when the Alq_3 coverage of Co was increased from 1 to 4 ML. Furthermore, by accounting for polarization effects, it is also possible to explain qualitatively the smaller TG found with STM. This is likely to be caused by a further change in the IP and EA as the STM measurements probe the TG gap for molecules *near the metallic interface underneath the organic film* [68,69]. Finally, we also point out that these STM estimates are consistent with the observation that, in studies about OLEDs, the TG of Alq_3 molecules at the interface with the electrodes is generally considered equal to about 3–3.5 eV as, otherwise, no charge injection into the Alq_3 layer would be possible with a TG as large as 5–6 eV.

Secondly, one additional reason for why the theoretical IP and EA are not expected to compare exactly to the UPS/IPS peak maxima is that in Alq_3 the HOMO, HOMO-1, and HOMO-2 have a relatively small energy separation, which cannot be resolved through photoemission (see Fig. 2). Then, the maximum of the UPS spectra peak, generally referred to as "the HOMO," is located at an energy that represents the average energy of the three highest occupied states, and as such, should be compared to the average energy of the three G_0W_0@PBE0 HOMOs. This average is equal to -6.95 eV for gas-phase Alq_3. Thus once the average IP $= 6.95$ eV is corrected by about 0.75 eV in order to account for the film-surface polarization [60], it becomes 6.2 eV, a value close enough to the experimental IP inferred by looking at the UPS HOMO peak maximum [9]. Similar arguments also apply to the interpretation of the first IPS peak, usually called "the experimental LUMO." In fact, this peak also originates from three closely energy-separated states (LUMO, LUMO+1, and LUMO+2), which cannot be resolved in spectroscopic measurements. The average gas-phase G_0W_0@PBE0 energy for these three states is -0.6 eV to be compared to the energy of the G_0W_0@PBE0 LUMO alone, which is equal to -0.8 eV.

In summary we argue that, in Alq_3, the TG evaluated by looking at the peak maxima separation is only a first approximation to the "real" TG, which is slightly smaller. The peak to peak approach may rather account for the gap between the average energies of the first three HOMOs and of the first three LUMOs. Finally, we must stress that the results, obtained by measuring the onset of the first UPS/IPS peaks, do not represent accurate estimates of TG either. In fact these will always be lower limits to the real TG: Even after neglecting the instrumental broadening, the onset values are affected by the broadening of the quasiparticle states resulting from the electronic coupling, the electron-electron interaction, the interaction with phonons, etc. Furthermore, the absence of a long-range structural order in the organic films produces an inhomogeneous broadening of the spectral features in the photoemission experiments (in the range of 0.7 eV in Ref. [76]), or equivalently give rise to the variation of the position of the injection level for electrons on different spots of the sample in scanning tunneling spectroscopy experiments (0.7 eV in Refs. [68,69]).

In conclusion, although our reasoning is based on the strong assumptions that (1) G_0W_0 provides a quite reliable estimate for the gas-phase IP (this is often the case for other molecules whose gas-phase IP is experimentally known), that (2) polarization effects are not negligible (this is a quite established concept [61,62,71] although it has been recently questioned [66]), and that (3) the figures of merit provided in Refs. [60,62] are fairly close to the real values, we are then able to provide some plausible arguments, which may reconcile a large set of theoretical as well as experimental discrepant data for the TG of Alq_3.

V. CONCLUSIONS

We have investigated in detail the electronic structures of four metal quinoline molecules with relevant applications in both organic optoelectronics and spintronics. Several theoretical methods, ranging from DFT to G_0W_0, have been employed. In agreement with previous studies about OSCs, we found that the molecules' DOS, calculated with the hybrid functional PBE0, represents in general a good first approximation to the occupied quasiparticle spectrum. However, in the interesting case of the novel $Al(OP)_3$ complex, we have pointed out how the PBE0 spectrum can differ from the G_0W_0 for states lower than the first ten HOMOs and how a direct comparison with the existing experimetal data is rather difficult owing to the large homogeneous and inhomogeneous broadening of the UPS spectrum. Finally, starting from our theoretical estimates for the transport gap of Alq_3, we have proposed a rational interpretation of the scattered and diverse data available in literature.

ACKNOWLEDGMENTS

A.D. would like to thank V. A. Dediu and V. Meded for useful discussions and S. Steil for providing the UPS data. Computational resources were provided by Trinity Centre for High Performing Computing (TCHPC) and Irish Centre for

High-End Computing (ICHEC). The research leading to these results was financially supported by the EU project NMP3-SL-2011-263104 HINTS. S.S. thanks the European Research Council for additional support (QUEST project).

[1] *Organic Electronics: Materials, Manufacturing and Applications*, edited by H. Klauk (Wiley-VCH, Weinheim, Germany, 2006).
[2] *Physics of Organic Semiconductors*, edited by W. Brütting and C. Adachi (Wiley-VCH, Weinheim, Germany, 2012).
[3] V. Dediu, L. E. Hueso, I. Bergenti, and C. Taliani, Nat. Mater. **8**, 707 (2009).
[4] S. Sanvito, Chem. Soc. Rev. **40**, 3336 (2011).
[5] C. Boehme and J. M. Lupton, Nat. Nanotechnol. **8**, 612 (2013).
[6] G. Szulczewski, S. Sanvito, and M. Coey, Nat. Mater. **8**, 693 (2009).
[7] V. Dediu, M. Murgia, F. C. Matacotta, C. Taliani, and S. Barbanera, Solid State Commun. **122**, 181 (2002).
[8] L. Nuccio, M. Willis, L. Schulz, S. Fratini, F. Messina, M. D'Amico, F. L. Pratt, J. S. Lord, I. McKenzie, M. Loth, B. Purushothaman, J. Anthony, M. Heeney, R. M. Wilson, I. Hernandez, M. Cannas, K. Sedlak, T. Kreouzis, W. P. Gillin, C. Bernhard, and A. J. Drew, Phys. Rev. Lett. **110**, 216602 (2013).
[9] A. Droghetti, S. Steil, N. Großmann, N. Haag, H. Zhang, M. Willis, W. P. Gillin, A. J. Drew, M. Aeschlimann, S. Sanvito, and M. Cinchetti, Phys. Rev. B **89**, 094412 (2014).
[10] S. Müller, S. Steil, A. Droghetti, N. Großmann, S. Sanvito, V. Meded, A. Magri, B. Schäfer, O. Fuhr, M. Ruben, M. Cinchetti, and M. Aeschlimann, New. J. Phys. **15**, 113054 (2013).
[11] P. Shakya, P. Desai, M. Somerton, G. Gannaway, T. Kreouzis, and W. P. Gillin, J. Appl. Phys. **103**, 103715 (2008).
[12] P. E. Burrows, L. S. Sapochak, D. M. McCarty, S. R. Forrest, and M. E. Thompson, Appl. Phys. Lett. **64**, 2718 (1994).
[13] V. Meded (private communication).
[14] A. Curioni, M. Boero, and W. Andreoni, Chem. Phys. Lett. **294**, 263 (1998).
[15] A. DeMasi, L. F. J. Piper, Y. Zhang, I. Reid, S. Wang, K. E. Smith, J. E. Downes, N. Peltekis, C. McGuinness, and A. Matsuura, J. Chem. Phys. **129**, 224705 (2008).
[16] F. Bisti, A. Stroppa, M. Donarelli, S. Picozzi, and L. Ottaviano, Phys. Rev. B **84**, 195112 (2011).
[17] M. Levy, J. P. Perdew, and V. Sahni, Phys. Rev. A **30**, 2745 (1984).
[18] C. O. Almbladh and U. von Barth, Phys. Rev. B **31**, 3231 (1985).
[19] J. P. Perdew, R. G. Parr, M. Levy, and J. L. Balduz, Phys. Rev. Lett. **49**, 1691 (1982).
[20] J. P. Perdew and M. Levy, Phys. Rev. B **56**, 16021 (1997).
[21] L. Kronik and S. Kümmel, Top. Curr. Chem. (2014).
[22] T. Körzdörfer, S. Kümmel, N. Marom, and L. Kronik, Phys. Rev. B **79**, 201205(R) (2009); **79**, 129903(E) (2009).
[23] J. P. Perdew and A. Zunger, Phys. Rev. B **23**, 5048 (1981).
[24] S. Kümmel and L. Kronik, Rev. Mod. Phys. **80**, 3 (2008).
[25] R. D. Adamson, J. P. Dombroski, and P. M. W. Gill, J. Comput. Chem. **20**, 921 (1999).
[26] T. Leininger, H. Stoll, H.-J. Werner, and A. Savin, Chem. Phys. Lett. **275**, 151 (1997).
[27] R. Baer and D. Neuhauser, Phys. Rev. Lett. **94**, 043002 (2005).
[28] T. Stein, H. Eisenberg, L. Kronik, and R. Baer, Phys. Rev. Lett. **105**, 266802 (2010).
[29] C. D. Pemmaraju, T. Archer, D. Sanchez-Portal, and S. Sanvito, Phys. Rev. B **75**, 045101 (2007).
[30] A. Filippetti, C. D. Pemmaraju, S. Sanvito, P. Delugas, D. Puggioni, and V. Fiorentini, Phys. Rev. B **84**, 195127 (2011).
[31] C. Toher and S. Sanvito, Phys. Rev. Lett. **99**, 056801 (2007).
[32] A. Droghetti and S. Sanvito, Phys. Rev. Lett. **107**, 047201 (2011).
[33] C. D. Pemmaraju, I. Rungger, X. Chen, A. R. Rocha, and S. Sanvito, Phys. Rev. B **82**, 125426 (2010).
[34] M. S. Hybertsen and S. G. Louie, Phys. Rev. B **34**, 5390 (1986).
[35] L. Hedin, Phys. Rev **139**, A796 (1965).
[36] G. Onida, L. Reining, and A. Rubio, Rev. Mod. Phys. **74**, 601 (2002).
[37] F. Aryasetiawan and O. Gunnarsson, Rep. Prog. Phys. **61**, 237 (1998).
[38] F. Hüser, T. Olsen, and K. S. Thygesen, Phys. Rev. B **87**, 235132 (2013).
[39] I. A. Sarsari, C. D. Pemmaraju, H. Salamati, and S. Sanvito, Phys. Rev. B **87**, 245118 (2013).
[40] M. Palummo, C. Hogan, F. Sottile, P. Bagala, and A. Rubio, J. Chem. Phys. **131**, 084102 (2009).
[41] X. Blase, C. Attaccalite, and V. Olevano, Phys. Rev. B **83**, 115103 (2011).
[42] P. Umari, G. Stenuit, and S. Baroni, Phys. Rev. B **81**, 115104 (2010).
[43] G. Stenuit, C. Castellarin-Cudia, O. Plekan, V. Feyer, K. C. Prince, A. Goldoni, and P. Umari, Phys. Chem. Chem. Phys. **12**, 10812 (2010).
[44] X. F. Qian, P. Umari, and N. Marzari, Phys. Rev. B **84**, 075103 (2011).
[45] C. Faber, C. Attaccalite, V. Olevano, E. Runge, and X. Blase, Phys. Rev. B **83**, 115123 (2011).
[46] N. Dori, M. Menon, L. Kilian, M. Sokolowski, L. Kronik, and E. Umbach, Phys. Rev. B **73**, 195208 (2006).
[47] N. Marom, X. Ren, J. E. Moussa, J. R. Chelikowsky, and L. Kronik, Phys. Rev. B **84**, 195143 (2011).
[48] T. Körzdörfer and N. Marom, Phys. Rev. B **86**, 041110(R) (2012).
[49] N. Marom, F. Caruso, X. Ren, O. T. Hofmann, T. Körzdörfer, J. R. Chelikowsky, A. Rubio, M. Scheffler, and P. Rinke, Phys. Rev. B **86**, 245127 (2012).
[50] V. Blum, R. Gehrke, F. Hanke, P. Havu, V. Havu, X. Ren, K. Reuter, and M. Scheffler, Comput. Phys. Commun. **180**, 2175 (2009).
[51] X. Ren, A. Sanfilipo, P. Rinke, J. Wieferink, A. Tkatchenko, K. Reuter, V. Blum, and M. Scheffler, New J. Phys. **14**, 053020 (2012).
[52] J. P. Perdew, K. Burke, and M. Ernzerhof, Phys. Rev. Lett. **77**, 3865 (1996).
[53] J. P. Perdew, K. Burke, and M. Ernzerhof, Phys. Rev. Lett. **78**, 1396 (1997).

[54] C. Adamo and V. Barone, J. Chem. Phys. **110**, 6158 (1999).
[55] V. Havu, V. Blum, P. Havu, and M. Scheffler, J. Comput. Phys. **228**, 8367 (2009).
[56] N. Marom, J. E. Moussa, X. G. Ren, A. Tkatchenko, and J. R. Chelikowsky, Phys. Rev. B **84**, 245115 (2011).
[57] AIMS manual, aimsclub.fhi-berlin.mpg.de.
[58] H. N. Rojas, R. W. Godby, and R. J. Needs, Phys. Rev. Lett. **74**, 1827 (1995).
[59] V. E. Henrich, X. Li, and Z. Zhang, J. Electron. Spectrosc. Relat. Phenom. **63**, 253 (1993).
[60] I. G. Hill, A. Kahn, Z. G. Soos, and R. A. Pascal, Jr., Chem. Phys. Lett. **327**, 181 (2000).
[61] N. Sato, K. Seki and H. Inokuchi, J. Chem. Soc. Faraday Trans. 2 **77**, 1621 (1981).
[62] I. G. Hill, A. J. Mäkinen, and Z. H. Kafafi, J. Appl. Phys. **88**, 889 (2000).
[63] E. V. Tsiper, Z. G. Soos, W. Gao, and A. Kahn, Chem. Phys. Lett. **360**, 47 (2002).
[64] R. O. Jones and O. Gunnarsson, Rev. Mod. Phys. **61**, 689 (1989).
[65] R. L. Martin, J. D. Kress, I. H. Campbell, and D. L. Smith, Phys. Rev. B **61**, 15804 (2000).
[66] S. Krause, M. B. Casu, A. Schöll, and E. Umbach, New J. Phys. **10**, 085001 (2008).
[67] A. Khan, N. Koch, and W. Gao, J. Polym. Sci., Part B: Polym. Phys. **41**, 2529 (2003).
[68] S. F. Alvarado, L. Libioulle, and P. F. Seidler, Synth. Met. **91**, 69 (1997).
[69] S. F. Alvarado, L. Rossi, P. Müller, P. F. Seidler, and W. Riess, IBM J. Res. Dev. **45**, 89 (2001).
[70] S. Sharifzadeh, A. Biller, L. Kronik, and J. B. Neaton, Phys. Rev. B **85**, 125307 (2012).
[71] S. Refaely-Abramson, S. Sharifzadeh, M. Jain, R. Baer, J. B. Neaton, and L. Kronik, Phys. Rev. B **88**, 081204(R) (2013).
[72] A. Droghetti and S. Sanvito (unpublished).
[73] J. B. Neaton, M. S. Hybertsen, and S. G. Louie, Phys. Rev. Lett. **97**, 216405 (2006).
[74] J. M. Garcia-Lastra, C. Rostgaard, A. Rubio, and K. S. Thygesen, Phys Rev. B **80**, 245427 (2009).
[75] A. M. Souza, I. Rungger, C. D. Pemmaraju, U. Schwingenschloegl, and S. Sanvito, Phys. Rev. B **88**, 165112 (2013).
[76] S. Steil, N. Großmann, M. Laux, A. Ruffing, D. Steil, M. Wiesenmayer, S. Mathias, O. L. A. Monti, M. Cinchetti, and M. Aeschlimann, Nat. Phys. **9**, 242 (2013).